

MODELLING THE EFFECTS OF MICROSTRUCTURE AND MICROTEXTURE ON THE STATISTICS OF SHORT FATIGUE CRACK GROWTH

Angus J. Wilkinson

Department of Materials, University of Oxford,
Parks Road, Oxford, OX1 3PH, UK
angus.wilkinson@materials.oxford.ac.uk

ABSTRACT

A physically based model for the growth of short fatigue cracks through a local grain structure will be presented. The growth rate is evaluated using an existing solution for the distribution of dislocations ahead of a crack in a slip band that is blocked by a grain boundary. Probability functions describing the grain size and grain orientation distributions are used within a Monte-Carlo framework so as to calculate the growth rates of many individual cracks passing through different local microtextures. The grain size controls the distance to the next barrier through which the slip band and crack must propagate. The grain orientations control the resolution of the far field tensile loading into shear stresses on local slip systems. It is assumed that the cracks grow along slip planes driven by the local mode II loading at rates that are proportional to the cyclic mode II displacement at the crack tip. Experiments show that the twist component of the crack plane deflection at a grain boundary is also of significance, since the crack retardation tends to be more marked for large twist deflections. The strengths of the microstructural barriers are thus controlled by the misorientation between the two neighbouring grains. The spatial distribution of grain orientations thus also enters the simulation. The simulations allow probabilistic descriptions of the microstructure and microtexture to be incorporated in a model that evaluates not only the average behaviour of the short cracks, but also the statistical variation in the behaviour. Curves showing the probability of propagating cracks reaching a given crack length in a given number of cycles will be presented.

KEYWORDS

Fatigue, short fatigue cracks, texture, statistics

INTRODUCTION

The number of cycles required for a naturally initiated fatigue crack to grow to a size at which it threatens the structural integrity of an engineering component is often dominated by its early growth rate in a regime where the stress intensity factor range is low and the crack length is short. Extrapolation of data and/or models that adequately describe the behaviour of long fatigue cracks into the short crack regime generally results in non-conservative predictions due to the faster growth of short cracks under the same nominal driving force (ΔK). Additionally, short fatigue cracks show increased sensitivity to local material

microstructure, there being many reports of crack growth rates rising and falling as a grain boundary (or other microstructural feature) is approached and then passed by the crack tip [see 1 for examples].

Evidence that the crack growth rate of short fatigue cracks tends to be reduced when plastic deformation ahead of the crack is blocked by a grain boundary was provided by selected area channelling pattern studies [2]. Such an effect has been modelled by Navarro and de los Rios and co-workers [3, 4] who extended the BCS dislocation modelling approach of Bilby, Cottrell and Swinden [5] in which the crack and the plastic zone ahead of it are represented by continuous distributions of dislocations. The extensive work of Navarro and de los Rios [6] analysed the retardation of the fatigue crack growth rate caused by the reduced amount of slip available when the plastic zone was blocked by a grain boundary. Such models successfully produce the observed pattern of rapid growth across a grain and retardation at the grain boundaries.

The scatter observed in the fatigue lives of samples that are nominally the same and cycled under the same loading conditions is in part due to the sensitivity of short fatigue crack growth rates to the local details of the microstructure. Boyd-Lee and King [7] have observed such effects in Ni-based superalloys, and developed empirical probabilistic laws to describe the of short fatigue crack growth that they could then use to predict the evolution of crack length populations through the fatigue life of a sample.

This paper examines the effect of preferred grain orientations (texture) on the statistics of short fatigue crack growth. The NR solutions given by Navarro and de los Rios [3] are used within a Monte-Carlo framework to follow the individual growth behaviour of many virtual cracks each sampling different possible local microtextures. From this the probability of a crack reaching a given length is obtained as a function of the number of load cycles.

THE MODEL

A schematic diagram illustrates the components of the model in figure (1). The sample is taken to be polycrystalline and subjected to a far field uniaxial cyclic loading (σ). In a plastically soft grain a crack forms on the active slip plane. The crack growth is assumed to result from irreversible shear deformation at the crack tip caused by the mode II component of the loading. The shear stress on the crack plane is assumed to be given simply by

$$\tau = \left(\frac{1}{1 + i_p - i_c} \right) \sum_{i=i_c}^{i=i_p} \frac{\sigma}{m_i} \quad \text{eq 1}$$

where m_i is the Sachs (single slip) orientation factor for the i th grain in the polycrystal. i_c and i_p are the grain numbers of grains containing the crack tip and head of the plastic zone respectively. The spatial distribution of grain orientations (relative to the loading axis) thus enters the model through equation 1.

The plastic zone ahead of the crack is described by BCS theory if the zone does not impinge upon the next grain boundary and by NR theory when the plastic zone is blocked by the next grain boundary. The crack growth rate is taken to be proportional to the cyclic displacement at the crack tip (Φ) for which equations 2a and 2b give results from the BCS and NR theories respectively.

$$\Phi_{\text{BCS}} = \frac{4b\tau_f c_{\text{BCS}}}{\pi^2 A} n_{\text{BCS}} \ln \left(\frac{1}{n_{\text{BCS}}} \right) \quad \text{eq 2a}$$

$$\Phi_{\text{NR}} = \frac{4b\tau_f c_{\text{NR}}}{\pi^2 A} \left\{ n_{\text{NR}} \ln \left(\frac{1}{n_{\text{NR}}} \right) + \sqrt{1 - n_{\text{NR}}^2} \left[\frac{\pi [1 - R] \tau}{4 \tau_f} - \arccos(n_{\text{NR}}) \right] \right\} \quad \text{eq 2b}$$

where b is the Burgers vector, τ_f is the friction stress resisting the forward motion of the dislocations within the grain (which is, of

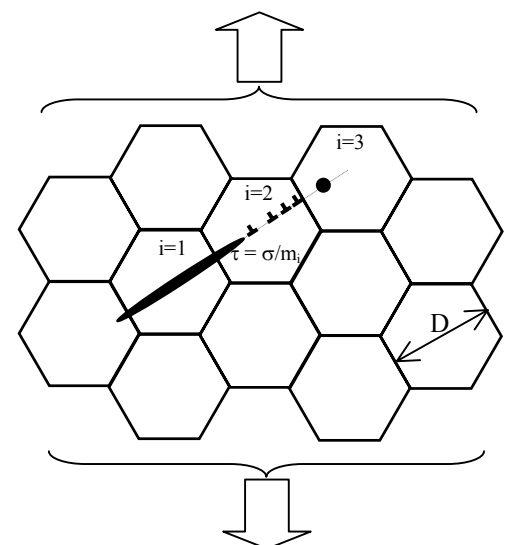


Figure 1: schematic diagram of the model

course, less than the macroscopic yield stress of the polycrystal), A is an elastic constant for the material ($A = \frac{\mu b}{2\pi(1-\nu)}$, with μ the shear modulus, and ν Poissons ratio). The applied stress (τ) and the load ratio (R) enter both theories through the parameter n , which is the ratio of crack length (a) to plastic zone size (c) as shown in figure 1. For the unblocked plastic zone the BCS theory gives

$$\frac{a}{c_{\text{BCS}}} = n_{\text{BCS}} = \cos\left(\frac{\pi[1-R]\tau}{4\tau_f}\right) \quad \text{eq 3}$$

while when the plastic zone is blocked its size is controlled by the position of grain boundaries, so

$$c_{\text{NR}} = \frac{D_1}{2} + \sum_{i=2}^{i=i_p} D_i \quad \text{and} \quad \frac{a}{c_{\text{NR}}} = n_{\text{NR}} \quad \text{eq 4}$$

where D_i are the diameters of the grains through which the crack has grown.

The plastic zone remains blocked at a given grain boundary until the stress $S(r_0)$ on a source a small distance r_0 into the next grain is sufficient to activate it, i.e slip is transferred when

$$S(r_0) \frac{m_i}{m_{i+1}} \geq S_{\text{crit}} \quad \text{eq 5}$$

The factor m_i/m_{i+1} is included to crudely accounts for the tilting of the slip plane in grain $i+1$ from that in grain i .

Calculation of the crack growth rate as a function of crack length a proceeds as follows:

- (i) calculate c_{BCS} and c_{NR} [eqs. 3 and 4]
- (ii) if $c_{\text{BCS}} > c_{\text{NR}}$ then calculate $S(r_0)$ and if condition [eq. 5] is satisfied increase i by 1 and start again from step (i)
- (iii) if $n_{\text{BCS}} < n_{\text{NR}}$ then growth rate is given by $\lambda \Phi_{\text{BCS}}$ [eq. 4] otherwise use $\lambda \Phi_{\text{NR}}$ [eq. 8]
- (iv) increase a to new value and repeat from step (i)

The parameter λ varies from 1 for completely irreversible slip, to 0 if slip is completely reversible.

As the crack grows from one grain to the next, sizes and orientations are assigned to the new grains using random numbers and probability laws that describe the overall grain size and orientation distributions for the polycrystal. The process is repeated for a large number of cracks so as to assess how the statistics of microstructure and texture impact on the scatter in fatigue behaviour.

RESULTS

Materials parameters typical of a peak aged Al-Li alloy (8090) will be used in the following illustration of the model. The values of the main parameters given in table 1 will be used unless explicitly stated otherwise. In all cases the simulations followed the growth of virtual cracks from an initial flaw size of $1 \mu\text{m}$ to a final length of $500 \mu\text{m}$ which typifies short crack growth leading to ‘initiation’ of an engineering crack.

TABLE 1
MATERIALS PARAMETERS USED IN THE CALCULATIONS

Parameter	Symbol	Value
Shear modulus	μ	29.6 GPa
Poisson ratio	ν	0.3
Burgers vector	b	0.286 nm
grain diameter	D	100 μm
Source position	r_0	1 μm
Source strength	S_{crit}	400 MPa
friction stress	τ_f	50 MPa
Slip reversibility	λ	0.05

Grain Size Distribution Effects

In polycrystalline metals and alloys the average grain size is a basic parameter often used to quantify the scale of the microstructure. However, considerable scatter in grain size about this average is often present, and more detailed quantified analysis typically leads to the representation of the population of grain sizes through a log-normal distribution. Figure 2a shows the cumulative fraction of cracks that have grown to a size of at least $500\ \mu\text{m}$ as a function of number of applied cycles at a stress amplitude of $200\ \text{MPa}$ ($R=0$), for simulated polycrystals with different grain size distributions shown in figure 2b. For each of these cases the crystal orientations have been assigned completely random orientations. Increasing the width of the grain size distribution from zero (thin line) is seen to cause increased spread in the fatigue behaviour as would intuitively be expected. Importantly the pronounced tail on the large grain size side of the log-normal distribution leads to the greatest changes being observed on the critical low-life part of the fatigue life distributions. Similar effects of an extended tail at low fatigue life are observed when the grain size distribution is altered to include a small fraction of ‘blown’ grains with markedly larger size outside the main distribution.

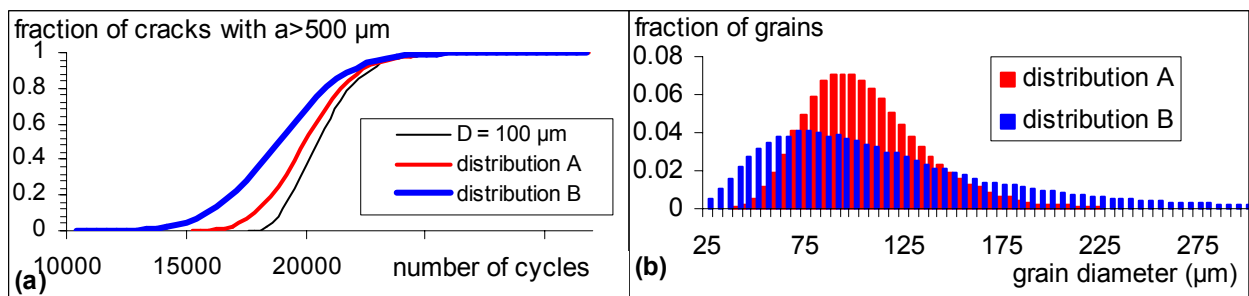


Figure 2: (a) distributions of fatigue cycles required to grow short fatigue crack to $500\ \mu\text{m}$ through grains with size distributions given in (b).

Grain Orientation Distribution Effects

The thin line in figure 2a shows that the specific grain orientations selected along a given crack path lead to a spread in the fatigue life even when the grain size is constant. The manufacture of the vast majority of engineering components involves some form of deformation processing (rolling, extrusion etc) and as a result quite marked preferred orientations or textures are imparted. In fcc metals textures involving the alignment of either $\langle 100 \rangle$ or $\langle 111 \rangle$ axes along the extrusion or rolling direction is relatively common. Figure 3a shows how these simple fibre textures affect the statistics of short fatigue crack growth. In each case the distributions of the misalignment angles between the $\langle 100 \rangle$ or $\langle 111 \rangle$ fibre axis and the loading axis was taken to be of gaussian form with a standard deviation of 10° . As before a stress amplitude of $200\ \text{MPa}$ ($R=0$), was used and the grain size was held constant at $100\ \mu\text{m}$. The differing preferred orientations result in considerable differences in both the average and the scatter in the fatigue life. The effects are more marked than those imparted by varying the grain size distribution (figure 2). Figure 3b shows how the variation in fatigue response is based on the Sachs factor (m_i) distributions present in the differently textured polycrystals. The randomly oriented (untextured) crystals have the lowest average Sachs factor and correspondingly the shortest average fatigue life, while the $\langle 111 \rangle$ fibre texture has the highest average Sachs factor (i.e. is plastically harder) and the longest fatigue life. The shape of the Sachs factor distribution also affects the calculated fatigue life distribution. For example, the untextured polycrystal results in a relatively small spread in Sachs factors with a pronounced tail towards the higher (plastically hard) Sachs factors and this results in a relatively narrow range of fatigue lives with a considerable part of this range taken up by the slowest 10% of the cracks. By contrast the wider range of Sachs factors present in the $\langle 111 \rangle$ fibre results in a broader range of fatigue lives.

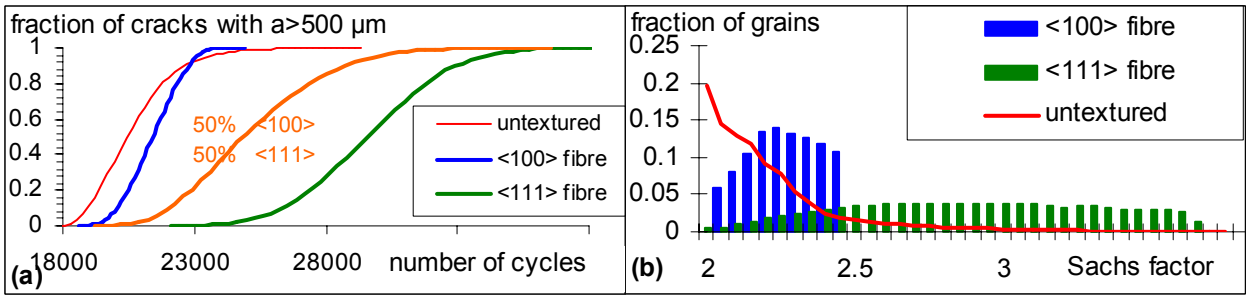


Figure 3: (a) distributions of fatigue cycles required to grow short fatigue crack to $500 \mu\text{m}$ through grains with different orientation distributions. (b) distributions of Sachs factors for different assumed textures.

Neighbouring Grain Orientation Effects

So far the calculations have been made on the basis that each grain boundary presents a barrier to the transfer of slip that is of the same strength. However, in reality the strength of the barrier will vary as a function of the grain boundary geometry, which leads to the observation that some grain boundaries cause a strong retardation (or even arrest) of short fatigue cracks while others have minimal effect. Recent experiments on Al-Li alloys [8] in which slip is highly planar and the cracks grow along $\{111\}$ slip planes have indicated that the crack propagation across a grain boundary tends to select the slip plane that will minimise the extent of crack plane twisting. Furthermore the strength of the crack retardation is greater at grain boundaries for which the minimum available twist deflection is relatively large. Here we define the twist angle $\Delta\Psi$ as the acute angle between the traces on the grain boundary of the slip planes in the two neighbouring grains.

The program was modified to incorporate such effects by rewriting equation 5 as

$$S(r_0) \frac{m_i}{m_{i+1}} \geq \left[1 + \frac{\Delta\Psi}{\Psi_0} \right] \frac{S_{\text{crit}}}{2} \quad \text{eq 6}$$

where Ψ_0 was set as 25° .

Furthermore, the slip system onto which the crack transferred across a grain boundary was selected by minimising

$$m_{i+1} \left[1 + \frac{\Delta\Psi}{\Psi_0} \right]$$

rather than simply minimising m_{i+1} , as was done in the previous calculations.

Any orientation coherence (i.e. any preferred spatial arrangement of the grain orientations) in the material would thus enter the model through two point correlations in the orientations which affect the distribution of $\Delta\Psi$ values in equation 6. However, in this work we will assume no such orientation coherence.

The effects of incorporating the sensitivity of grain boundary strength on the twist deflection of the crack plane is illustrated in figure 4. For a polycrystal with a <100> fibre texture the deflection of the crack plane as it crosses grain boundaries is generally rather limited since the grains all share similar orientation and as a result only a small increase in the width of the fatigue life distribution occurs. However, for an untextured polycrystal, the random sequence of grain orientations leads to more significant crack plane deflections at the grain boundaries and hence a wider range of grain boundary strengths. In this case the increased variability of the strength of crack retardation at the grain boundaries causes a marked widening of the fatigue life distribution. Furthermore, inclusion of the neighbouring grain orientation effect generally makes it easier for cracks to propagate through the <100> fibre textured material than the untextured material despite the <100> oriented grains being plastically harder.

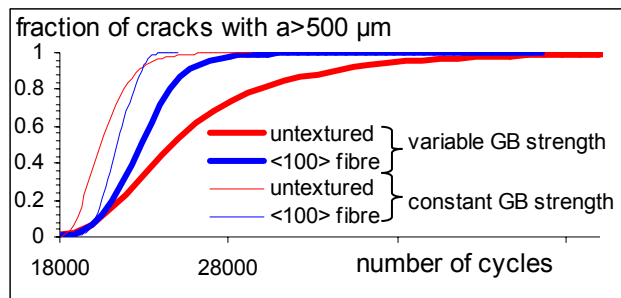


Figure 4: effects of variable grain boundary strength on the distributions of fatigue cycles required to grow short fatigue crack to 500 μm through grains with different orientation distributions.

CONCLUDING REMARKS

The characterisation of materials has seen a significant advance in the development of the automated electron back scatter diffraction technique [9], which allows the spatial distributions of grain orientations to be determined in a statistically significant way. It is important that models aimed at linking microstructure to material properties adopt frameworks allowing incorporation of statistical information describing grain size and grain orientation distributions and any spatial or other correlations between them. The modelling described in this paper is a simple step in this direction.

The physically based model for the growth of short fatigue cracks developed here allows the effects of grain size, grain orientation and neighbouring grain orientation distributions to be simulated within a Monte-Carlo framework. The simulations track the growth of many individual cracks through different possible paths through the microstructure and allow not only the average crack behaviour but also the statistical variation in the crack behaviour to be examined.

ACKNOWLEDGMENTS

I am grateful to the EPSRC for funding this work (GR/L48669) and to the Royal Society for their continuing support through the University Research Fellowship scheme. My thanks go to Drs Tongguang Zhai and John W Martin for insightful discussions about short fatigue crack growth.

REFERENCES

- 1 Suresh, S. and Ritchie, R. O. (1984) *Int. Metals Rev.*, **29**, 445-476.
- 2 Edwards, L. and Zhang, Y. H. (1994) *Acta Metall. Mater.*, **42**, 1423-1431.
- 3 Navarro, A. and de los Rios, E. R. (1988) *Phil. Mag. A*, **57**, 37-42.
- 4 de los Rios, E. R. and Navarro, A. (1990) *Phil. Mag. A*, **61**, 425-449.
- 5 Bilby, B. A., Cottrell A. H. and K. H. Swinden (1963) *Proc. Roy. Soc. Lond. A* **272**, 304.
- 6 de los Rios, E. R., Xin, X. J. and Navarro, A. (1994) *Proc. Roy. Soc. Lond. A*, **447**, 111-134.
- 7 Boyd-Lee, A. and King, J. (1993). In: *Fatigue Design (ESIS Publication 16)*, pp283-296, Solin, J., Marquis, G., Siljander, A. and Sipila, S., (Eds). Mechanical Engineering Publications, London.
- 8 Zhai, T, Wilkinson, A. J. and Martin, J. W. (2000) *Acta Mater.* **48**, 4917-4927.
- 9 "Electron Backscatter Diffraction in Materials Science" eds. Adams B. L., Schwarz A. J. and Kumar M., (Kluwer Academic/Plenum Publishers)